

Response 1

We would like to thank the reviewer for their helpful and detailed review. Our responses are bolded.

First of all, I would like to thank the authors for their contribution to the progress in the emergent field of cryo-seismology. Studies like this can help to improve and establish passive seismic methods for monitoring and better understanding glacier dynamics. (1) My main comment is that the method is actually not new in seismology or acoustics, but has been suggested as a simple graphical signal localization method before, e.g. in:

J. Pujol (2004)

[...]

I agree that this study presents the first application of this method to calving localization. However, this is not such a different approach compared to using traditional localization methods based on first onsets (without using S waves). Basic processing and assumptions are the same: you have to know the velocity model and to pick first arrival. Just using P wave onsets, it is necessary to use some constraints on source locations, but you do the same here when choosing one hyperbola.

The authors should clearly write this and state some references.

Thank you for pointing this out! We have now added the original hyperbolic method paper (Mohorovicic 1915) to the introduction and referenced Pujol (2004) who suggests that this method is best for shallow events where refraction along a bottom interface is insignificant.

(2) The title suggests a two-station method. This is true if the location of the terminus is known. However, in the paper the authors only present results of using more than two stations at Hellheim and Jakobshavn glacier (hyperbola intersection). So I would suggest to change the title or put more emphasize on two-station results in the paper.

We intended “two” to mean “pair-wise”, i.e. you need two stations to define each hyperbola. We have changed the title to “Calving Localization at Helheim Glacier Using Multiple Seismic Stations” for clarity and added “paired” to the abstract description.

(3) Determination of signal onsets for time differences : This is not explained clearly enough and it would be nice to provide more details. Define what “slope” is! Did you use the raw waveforms or the signal envelope? Any references for this method? Is it similar to STA/LTA? What is the time window around the pre-defined event used here? For such a low number of events, wouldn’t manual picking be more precise and feasible? Is the onset time the same that is used to compute V_{eff} ? I am a bit surprised that cross-correlation does not work. Have you tried to use only the first, more coherent part of signal, not the whole event? I would expect that cross-correlation is a much more precise measure of time lags than any automatic picking algorithm.

Added details: the slope is from the raw waveforms, and this method is entirely empirical. We were unwilling to do a manual method because this would be subjective, but our automated method still requires manual checking (and our 44% value was manually/empirically determined). The time window for cross-correlation was the 25s window pictured in Fig. 4. Cross-correlating the entire event doesn't work either, we suspect this is

because the same calving event can look very different at two different stations:

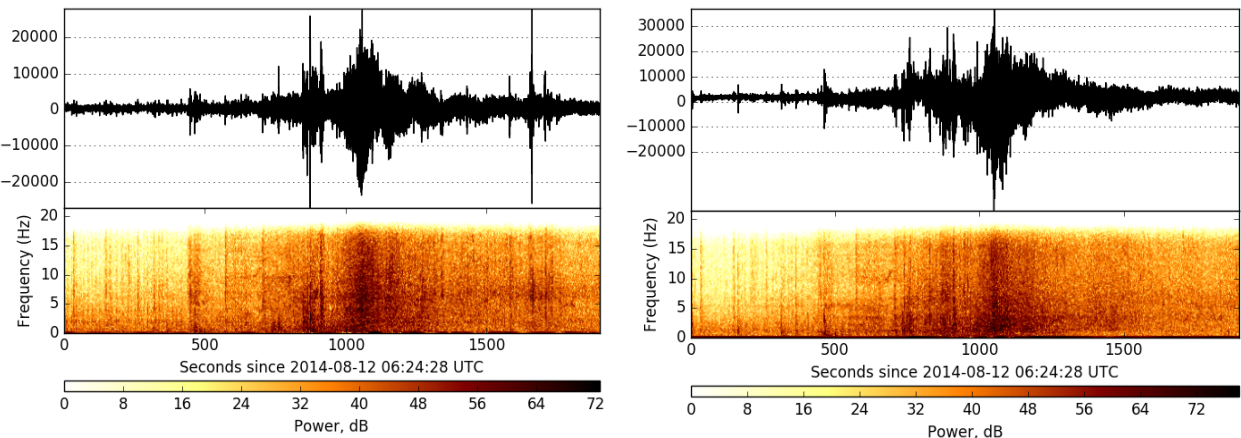


Fig. A1. The same calving event at two different stations.

These signals have such different shapes that cross-correlation does not work. It would probably work better with just the wave envelope, but to create that, there would probably be some rounding or other shift of at least 0.5s, which is significant as most of our lags are <3 s. It may be better just to state that we are manually detecting the events and using our automated 44% trigger to know what neighborhood to inspect.

Other comments:

page 1 line 12 : I would say the effect of calving is not just equal, but can also be larger than melting at individual glaciers.

Noted and changed.

page 2 line 2 : Calving seasonality in general is not only due to melange ice, but also due to increase in meltwater-induced sliding, ocean temperature variations, and ocean tides, etc ...

Noted and changed.

Page 2 line 16 – 21 : Other possible causes for seismic calving signals have been suggested (at least for calving styles observed in Alaska and Svalbard) : ice - sea-surface interactions (Bartholomaeus et al., 2012, in JGR; Köhler et al., 2015, in Polar Research).

Noted and changed.

Page 2 line 30 : Another possibility of locating complicated signals without using pre-determined velocities of individual seismic phases are the use of small-aperture arrays. Directional information can be obtained by applying signal beamforming or Frequency-Wavenumber analysis which can then be triangulated. (Köhler et al, 2015, in Polar Research; Koubova, 2015: www.duo.uio.no/handle/10852/45791?show=full)

Based on my reading of Köhler 2015, it seems like the method is manual phase-picking of P/S waves to generate a backazimuth and distance, as their array is regional and thus far enough to distinguish different phases? We have added Koubova's description of beamforming, though it seems to rely on having a backazimuth already (which we do not have in our case until after the location is determined).

Data section : Are all calving events used here detected manually or is an

automatic detector used? Are the calving events identified only based on inspection of frequency spectrum ? I would expect that regional earthquakes have energy above 1 Hz as well (see e.g. Köhler et al, Svalbard). Description of JIG station data is missing.

C3

The JIG data are now removed from the study as we should not reasonably expect that surface velocities are equivalent to Helheim. Events are detected semi-automatically using a Signal/Noise threshold then individually inspected to rule out regional earthquakes, which have different frequency breakdowns - see Figure A2.

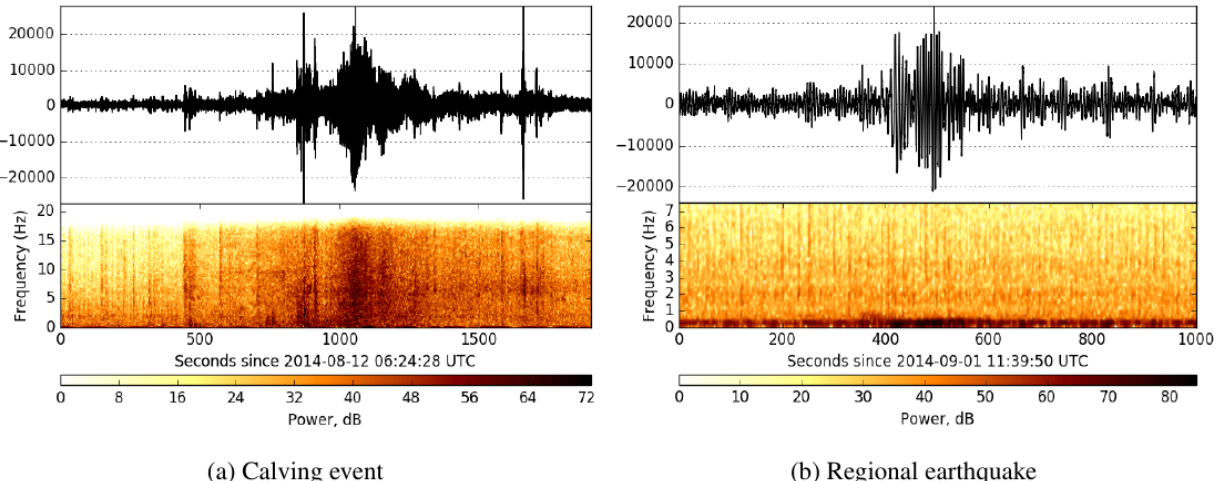


Fig. A2. The spectra (top) and spectrograms (bottom) for a calving event (a) and a regional earthquake in Iceland 960km away (b).

Page 3 line 15 : “teleseismic events from regional earthquakes” : Please rephrase : Either it is a teleseismic earthquake or a regional earthquake. In seismology there is a clear distinction between both events.

Thanks, noted. The earthquake is ~960km from the station which is very near the teleseismic threshold, but we have gone with just “regional” instead.

Page 6 Line 18 : What do you mean with “only two seismometers”. Is the signal too noisy on the others stations? If not, why not use all stations for a robust estimation of v_{eff} ? What are the individual measurements for all stations and all calving events? Is there really no difference between Hellheim and Jakobshavn?

“Only two seismometers” is because only two seismometers were deployed in August 2013-2014, and the other two seismometers were deployed after the calving event had occurred. What do you mean by “individual measurements of all stations”? The other calving events that form our catalog were not observed (though they were confirmed to be calving events using MODIS Terra satellite imagery). The Jakobshavn event has been removed because even if the velocities seem similar, it may be coincidental and we should not give any weight to the Jakobshavn data.

Fig 5 : Two hyperbolas are shown for each velocity. I suppose they correspond to two stations pairs. Which of the three possible station pairs to they correspond to? Why not plot all three hyperbolas? Also, indicating the exact location of calving front at the time of the calving event would be helpful. Then one could see how an

individual hyperbola intersects with the terminus. After all, this is what the authors suggest: a two-station method. It looks like $V_{eff}=1.4$ could be as good, or even closer to the front.

Furthermore, the authors write that the calving events appears to be in the ocean. However, it is actually located on the glacier (the melange is in the west, isn't it?). **Yes - the melange is actually west. Though, this plot has been removed in any case (we are removing all references to Jakobshavn).**

Page 7 line 3 : "teleseism", write teleseismic earthquakes, see my comment about regional earthquakes above

Noted, thanks

Discussion about velocity: What about the more distant station at Jakobshavn (JIG 1 and 2)? The signal would have to travel through a lot of rock (possibly at sea bottom) I guess.

Removed Jakobshavn event.

Discussion about depth: I am not sure if the main limitation for depth resolution is the missing velocity model for the glacier. One simply needs more stations close and above the source (on-ice) for a more precise and accurate localization. Also, I actually don't see the need to determine the depth of calving. Calving is usually affecting the whole height (or a big part) of the terminus (except maybe submarine events or small pieces of ice). However, I agree that depth may be relevant to analyze precursor events like fracturing.

Our reviewer #3 pointed out that depth is not a well-posed question - for an event that removes an entire column of ice, there is no real 'depth' (unless you use the depth of the entire glacier, which is measurable with bathymetry). We will minimize the discussion of depth.

C4

Page 9 line 2: Even for a station at same elevation, P waves could come from below (refracted, diving waves).

True. For our study, we show that the wave arrivals are dominated by surface (Rayleigh) waves, and so we are able to neglect refracted/diving waves.

Brune model: I am not sure if this source model can be applied here. If calving signals are associate with a simple rupture process I would agree. However, many mechanisms have been suggested (ice-sea-surface interactions, interaction with fjord bottom, forces that cause change in the motion of the ice after and during calving (glacial earth- quakes at Hellheim, Murray et al, 2015)). I doubt that it is mainly the rupture signal that we see on the seismometers ...

Agreed - the Brune model was intended as a comparison to see if it were a rupture, what size it would be. Do you think we should not mention Brune at all, or qualify it more (that it may not be a rupture signal at all, but if it is, then it has size 50m)?

Fig. 8 : Can you indicate the front retreat on the map? Is it consistent with the event locations?

Updated figure. Figure A3 shows that the calving fronts are close to the events - a good check to make!

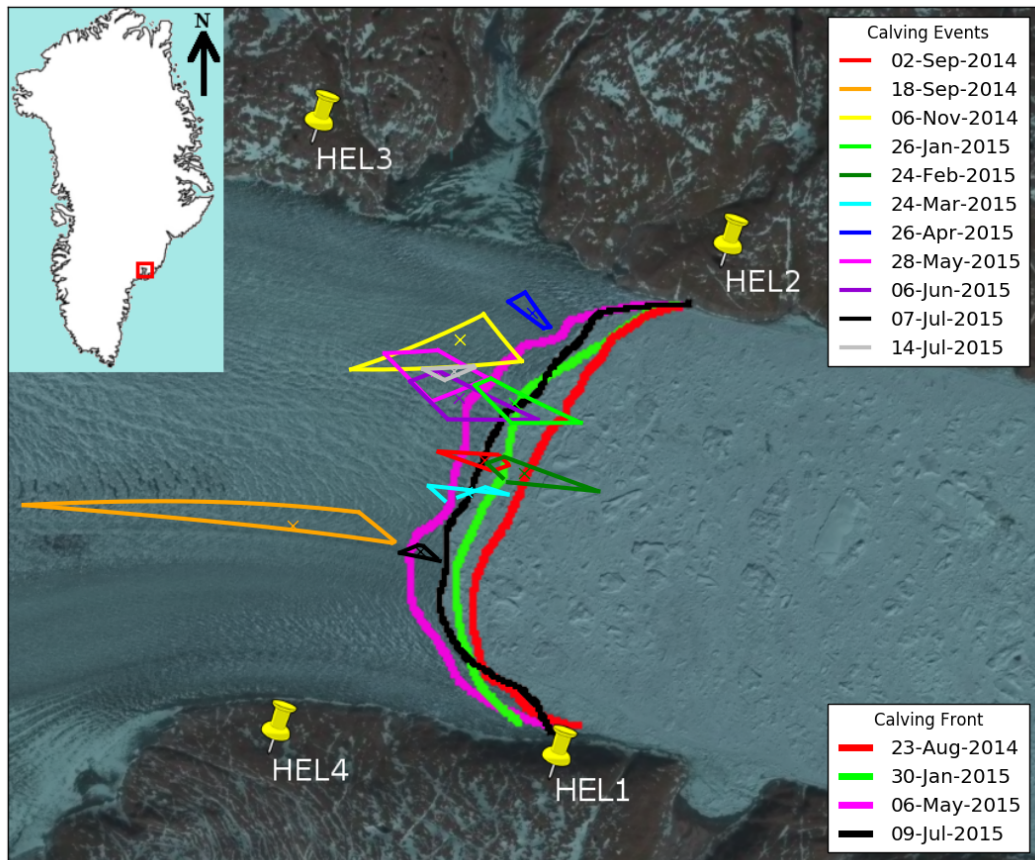


Figure A3. Catalogue of eleven calving events localized on Helheim glacier, showing the movement of the calving front for certain dates (taken from Landsat 8).

In Conclusion: "...get around the emergent P-wave problem" : I don't agree. You still have to deal with the emergent onset, i.e. to pick an arrival to determine the time lag (see comment above). That, and estimating the velocity, are basically the same tasks for traditional travel-time based localization methods

A fair point - we have changed this to "We find that the local seismic signals are dominated by surface (Rayleigh) waves, which makes distinguishing between different seismic wave components (a key benefit of regional arrays) irrelevant. A local array is able to localize calving with greater resolution than a regional array. Identifying the signal onsets is not fully automated and requires manual inspection of signals, due to the emergent signals involved in glacial calving."

Response 2

Thanks for your helpful comments! Our responses are **bolded**.

- When you attempted to cross-correlate the seismograms, did you use the entire seismogram (e.g., similar to what is shown in Figure 2) or just some subset of the seismogram? If the former, one issue that might cause problems is that calving events often involve the detachment of multiple icebergs. I would guess that the calving events shown in Figure 2 involved 2-3 icebergs. If the latter, how did you determine what subset to pick? Also perhaps show what section of data you are using, or refer to Figure 12 when describing the section of data that you used. Its not clear exactly what data you are using.

We cross-correlated the snippets like those in Fig. 12, which were manually chosen by looking at sharp peaks in the spectra. We required that all four stations had clear peaks (so that we could identify lags) - in some cases this was not possible. We have added text to clarify that we are using the windows in Fig. 12 in the cross-correlation.

- I understand that cross-correlating the seismograms did not give satisfactory results for the calculating the time delay. Did you also consider cross-correlating the envelope of the waveforms? I'm wondering if there is a more robust way of calculating the time constant that doesn't rely on an empirical constant.

Our reviewer #1 suggested just to manually pick out the lags due to the small sample size. We were not wanting to do it fully manually due to the inherent subjectivity. Cross-correlating the envelopes would lose the resolution of the lags as the envelope is of order 5 s (in Fig. 6) but we have lags of order 1-3 s or so and even a 0.5 s shift would dramatically change the hyperbola. We were unable to think of a truly automated way of calculating the lags - we could also do a STA/LTA method but all methods require manual checking to see if the results are sensible (like for cross-correlation, we found implausible lags). Do you think it would be better just to concede that even our most automated method requires manual verification, and to just scrap our empirical values and do the localization manually?

- This study focused on large, full-thickness calving events that occur on weekly timescales. These are events that, at least for focused studies on individual glaciers, can often be located using time-lapse or satellite imagery (as stated in the paper). Smaller calving events clearly occur more frequently. Admittedly, these smaller events may be insignificant for the total mass loss from glaciers like Helheim and Jakobshavn, but understanding the variability of these smaller events

may provide insights into processes driving calving. If you decrease the STA/LTA threshold, can you detect and locate more events? If so, what sort of patterns emerge?

The biggest issue here is that the lower-amplitude events have a smaller slope (because they have a lower amplitude change in more-or-less the same time time step) and so our automated lag detector is much less accurate. Moreover, as the peaks are less sharp, it's also harder to manually identify them. However, if there is relatively low noise around the signal, and there is a short, sharp burst (like at 03:06 in Fig A3 below), then our method does converge. But because calving signals are emergent, we don't have these short sharp bursts during the main calving event. So we are unlikely to be able to localize the main calving signal for small events, but we may be able to localize nearby secondary signals from these events - though this probably would not localize the calving event itself.

- Another way to expand the applicability of this method is to show that it works for regional seismic data. Full-thickness calving events at Jakobshavn Isbrae are detectable at ILULI (50 km away), SFJD (250 km away) and sometimes SUMG (400? km away), even when the calving events don't generate classic "glacial earthquakes". Have you tried incorporating regional seismic data into your method? Can a regional seismic network such as GLISN be used to detect and locate large calving events around Greenland (besides those that generate glacial earthquakes) using your methodology?

Kira Olsen presented a poster at AGU 2015 that looked at locating glacial earthquakes using GLISN (using an azimuthal method), though due to the distance of the seismometers, this localization was limited to identify which glacier calved and not where on each glacier the calving occurred. We do not believe our method easily scales up to regional arrays, as a key assumption (that the surface velocity is constant in all directions) is no longer valid with different travel paths from the epicenter - this means the locus would no longer be a hyperbola, but rather some (more complex) other shape. Also, at higher distances, the error in v_{eff} would make the localization too imprecise (likely over most of the glacier). Though, the main limitation is the lack of a constant v_{eff} . Another test for the validity of our method is to look at calving fronts and to see if our localization matches - and our method does hold (Figure A2 below).

A few more minor questions:

- The authors state that calving at Helheim preferentially occurs on the north side of the glacier. Is this where the glacier is thickest/fastest? Is this statement really just saying that full-thickness calving events only occur in that region?

This is where the glacier is thickest (Fig A2), by about 200 m.

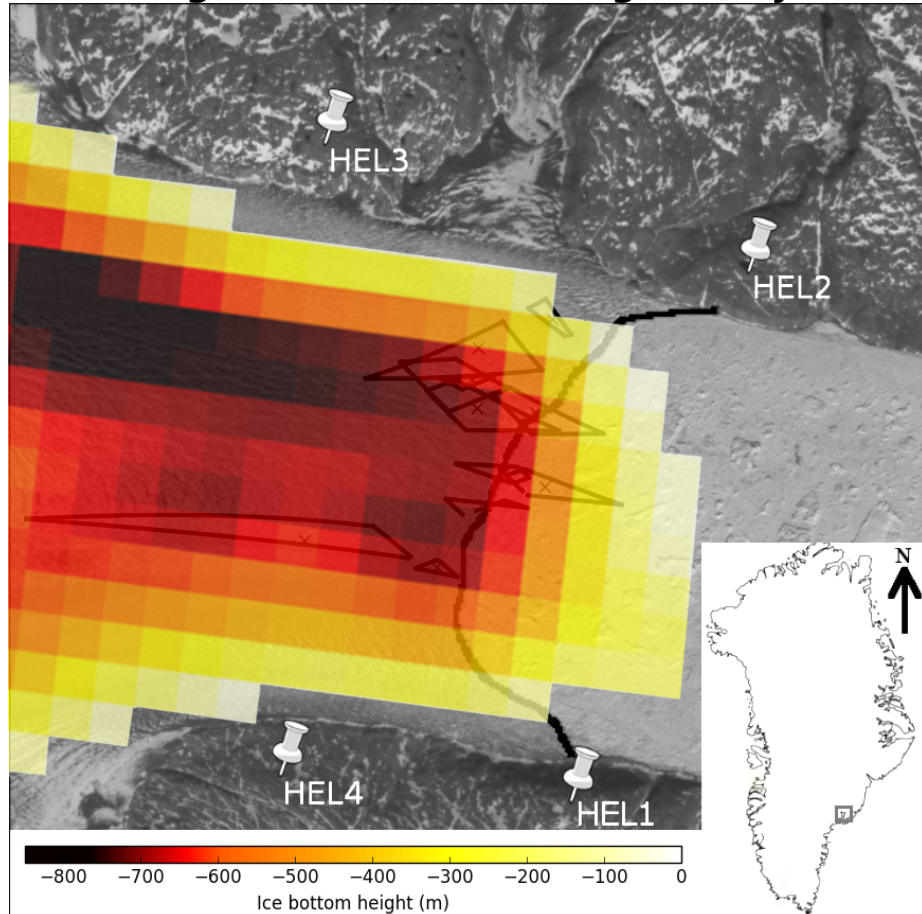


Fig A1. Topography of the rock below Helheim Glacier, taken from NSIDC McORDS flights collated between 2008-2012.

- What is the date on the googleearth imagery used in the figures? Perhaps it makes sense to use newer imagery that was captured closer to the time of study (e.g., from Landsat 8)?

Yes - we have now updated this (Fig A2) to use a Landsat image from July 2015, and we use three other images to also show the progression of the calving front (at the suggestion of reviewer #1).

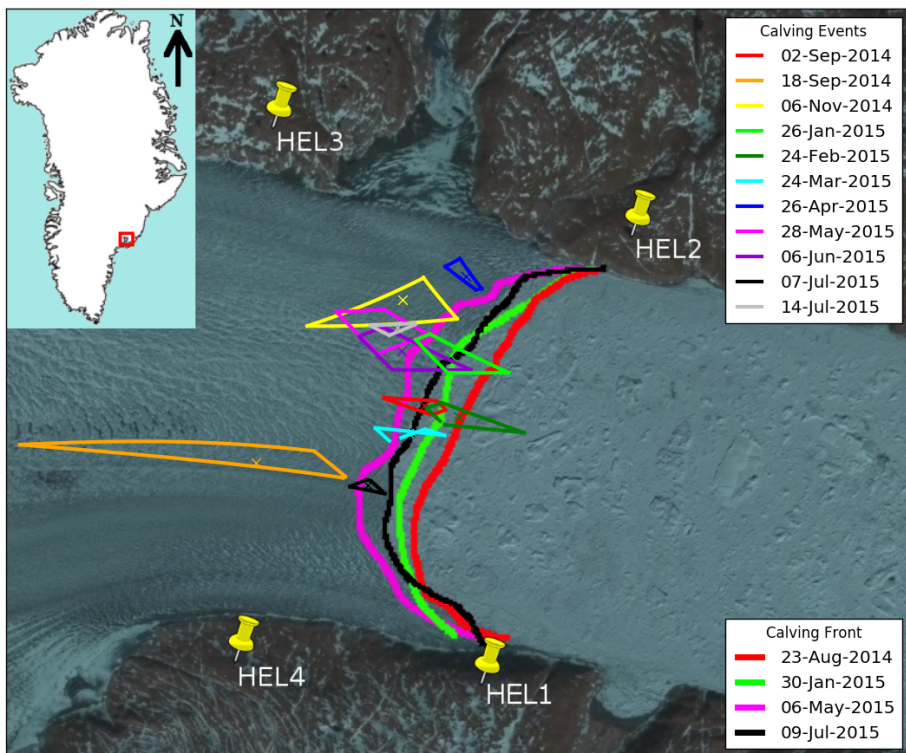


Fig. A2. Updated calving catalog showing locations and the movement of the calving front.

- I would guess that two or three icebergs calved during the events that appear in Fig. 2. What happens if you analyze each of the peaks in seismicity separately? Do you see calving propagating upglacier or across the glacier face?

The calving event Fig. 2 is from August 2014, when only two seismometers were available, so unfortunately we are unable to localize those events. However, we found another multiple-calving event (June 6 2015) which we treated the peaks separately (Fig. A3). It looks like the calving progression in that figure goes Red, Yellow, then it splits in two directions and goes Blue-Purple and Green. The estimated calving localizations all touch the calving front of June 5 (from Landsat), which is good. Do you think this plot is worth adding to the manuscript? This event is part of the calving catalogue from the manuscript you already saw, but only the “main” event (i.e. the highest peak at 2:30) is used. The plot may be a bit misleading because the shapes may suggest calving magnitude, which is not the case here (the biggest area in purple actually represents the smallest amplitude signal).

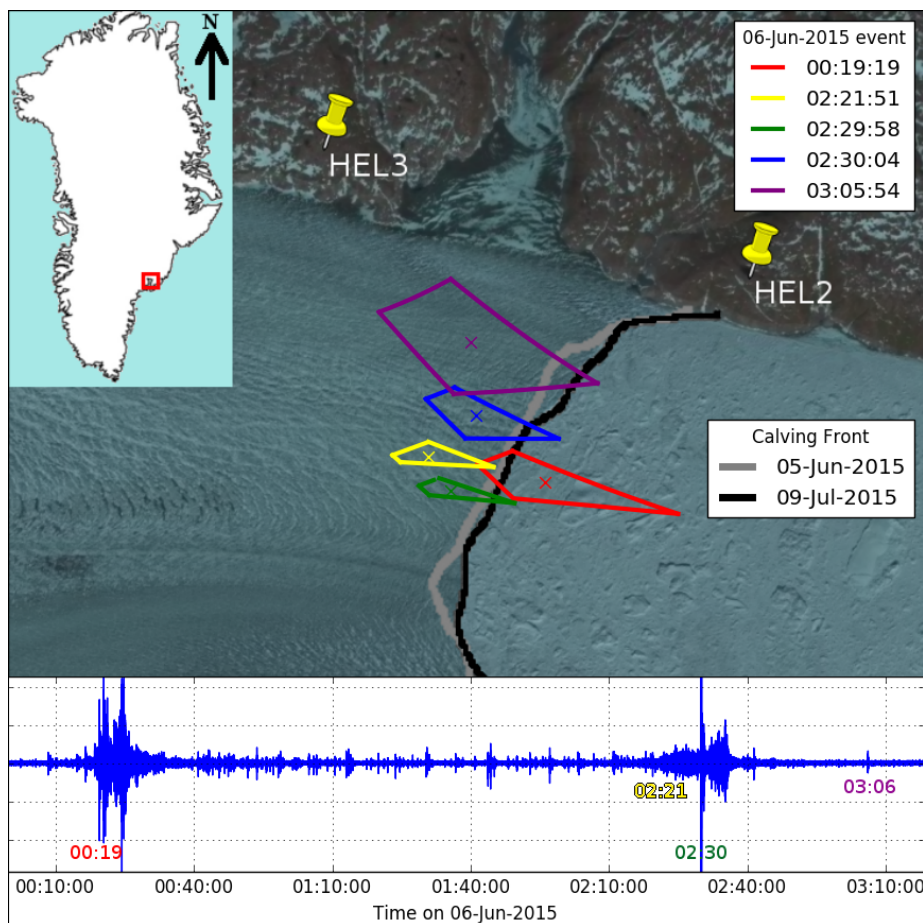


Fig A3. Multiple-iceberg calving event on June 6 2015.

- page 9, equation for radius of a circular fault: the equation contains β_0 , but the text describing the variables only refers to β . Should these be the same thing?

Yes - thanks.

Response 3

Mei et al. analyze passive source seismic data mainly from Helheim glacier to localize calving events. For the localization they pick the first arrival of the seismic signal of the calving event. Combined with a predetermined velocity hyperbolas are calculated to determine the source location. This method is used for calving events at Helheim between Sep 2014 and Jul 2015, localizing 11 events in total. Finally, the authors use these events to determine the size of the calving event and speculate that the clustering of the calving events on the northern half of Helheim might be due to larger ice thickness and differences in surface roughness. The paper uses a seismic method not applied for the localization of calving events before. It is great to see a different method applied to the subject of localizing calving events from nearby seismometers.

The paper is in most parts easy to understand. The method should be explained in a bit more detail in certain parts and I do have some questions regarding the validity on how the method is applied here.

Thank you for your extremely detailed review. Our responses are in bold.

General comments:

It is not a hundred present clear to me, what the main focus of the paper is. Is it to introduce the hyperbolic method for the localization of calving events and Helheim glacier is just an example of the application of this method, or is it the localization and interpretation of the calving events for which the hyperbolic method is introduced? I think that should be clarified and the text adjusted accordingly.

After we learned from review 1 that the hyperbolic technique is already used in acoustics/seismology (but not yet for glacial calving), we have shifted the focus of the paper to the localization and interpretation of calving events for which we use the hyperbolic method (and also a grid search method as you suggest). Our revision of the manuscript hopefully reflects this better.

You use a lot of fill words and subjective descriptions, that make sentences unnecessarily long (also, some, severely, powerful). Readability and understandability would increase significantly if the sentences were shorter and the sentence structure less complex. Often it would be easy to split one sentence into two sentences.

Thanks. We have gone through the manuscript to try and break up long sentences.

Chapter 3 Hyperbolic Method: I do have some question regarding the method: - Why does the cross correlation not work? Are the waveforms so different due to the difference in interference of the different wave types at the different stations? Could you please clarify this? Did you try different bandpass filters and window length for the cross correlation. **We believe cross-correlation does not work because the signals sometimes look very different in different directions. This may be due to the orientation of the fracture. There is no clear pattern to which pairings do not have successful cross-correlation. Possibly this is also because when the calving event happens, the icebergs are formed on the eastern side, and this is non-symmetric to the western side so the signal is not radially identical. It is also possible, as you state, that there is interference from linearly polarized waves (e.g. the P-wave) that affect the shape of the waveforms at each station differently. We tried different filters both for high and low and both for the overall waveform shape and for the small peaks, but we could not get good values for all events and all seismometer pairings, and as a result we could not use this fully automated method.**

-How big is the error when you pick the first arrival (estimate), what does this mean for the precision of your localization?

So the estimate of the lag (i.e. a subtraction of the arrivals) should have any systematic

error removed by the subtraction. One reason we did not want to pick out arrivals by eye is because of the error that this would create. The random error of the actual estimation is hard to quantify as the true arrival is not known. Signal onset detection is still an ongoing area of research (e.g. Ross & Ben-Gurion 2014). One way to quantify the error is to use the error of localization (compared to camera-observed events) and then reverse-engineer the time lag.

Ross, Z. E., & Ben-Zion, Y. (2014). Automatic picking of direct P, S seismic phases and fault zone head waves. *Geophysical Journal International*, 199(1), 368-381.

- If you do not determine the wave type how can you be sure that the first break you are picking is coherent. Most likely and in most cases you will pick the surface wave. Which would be totally valid, and you later state that it is the surface wave you are analyzing. So why not determine the phase you are using for the analysis and use surface waves. My fear with this technique is that you might have a seismometer close to the source and it is not possible to see the P-wave first arrival, so you would pick the surface wave. For a seismometer that is further away the P-wave and surface wave might be separated better, hence the wave you pick would be the P-wave. But if you pick different wave phases at different stations how do you want to use one velocity to find the correct location of your source. Imagine you pick the P-wave at seismometer 1 and the surface wave at seismometer 3. For the analysis you then use the velocity of 1.17 km/s, your localization would be totally wrong. This is a crucial point and the way I understand your analysis I can't see that the analysis is correct as you apply it. Please clarify this!

This is a good point. For our method, we checked all the particle plots for each event to conclude that they are all dominated by surface (Rayleigh) waves. We originally thought it fit better in the Discussion of what waves were being detected, but this analysis was done before making the localization catalog. We agree it is important as a premise for our technique so we have moved this section to the Methods.

- How was the location of the calving events observed by persons determined. Where this events filmed? Small errors in the location of the observed calving events will lead to big errors in the derived velocity. How do you derive such a small error as 0.1 km/s? Please clarify how this velocity is determined in more detail.

The events were filmed, but you are right there could be small errors in the viewed localization, so we are changing our velocity estimation method. We used a grid search as you later suggest, and got a best fit of 1.20 +- 0.03 km/s. We have updated our plots (this changes the locations only slightly). 0.1 is the standard deviation of the best fit velocities for our 11 events, and so the standard error for these 11 points would be $0.1/\sqrt{11} = 0.03$ km/s.

- How can you use the data from Jacobshavn to determine the velocity. It's a completely different setting then Helheim. At Helheim your seismometers are located inland of the glacier front, i.e., waves will travel a large part through glacier ice. At Jacobshavn the seismometer are located, mostly (except of seismometer 3), downstream of the glacier front, i.e. waves mainly travel through water and ice mélange. You must derive totally different velocities for these two locations.

Yes, you are right. We have deleted this section and determined our velocity using grid search with Helheim only.

- Did you try a grid search. As you do have multiple seismometers you could use the derived lag of all combination and find the global maximum testing different directions and velocities.

Thanks for this suggestion. We applied a grid search, as mentioned above, successfully.

Discussion: Large parts of the Discussion are not a discussion but an interpretation of the results or even speculation of what their causes are. This needs to be clearly differentiated, discussion and interpretation.

We have now separated into an “interpretation of results” and a “discussion of methods” subsection.

Determination of magnitude: For the method of Brune, you say, you have to use the corner frequency of the S-wave. But you don't use the S-wave, so why should that method be valid here at all. Further, I have trouble seeing the corner frequency between 1-5 Hz in your plots in Fig. 12. And why do you choose this small time interval you are using for the calculation of this spectrum?

This method is intended as a comparison of traditional seismic techniques to see what a fracture size would be following the Brune model. The S-wave velocity is needed for this, and we do not have S-waves as you mention, but we use the relationship between S-wave speed and surface wave speed (as a function of the Poisson ratio) to estimate the S-wave velocity. The small time interval is because we believe the high-amplitude peak corresponds to the main calving event, and so we want to estimate the fracture size from this particular window.

Figures: Must appear in the order in which they appear in the Text. Fig 6 – page 6 line 6, Fig 5 – page 6 line 20. Always refer to the Figure by number, not see the above Figure. It is not necessary to write (see Figure...) instead (Figure...) is sufficient. It is totally clear that I'm supposed to have a look at the Figure.

Thanks for this, we have checked the order carefully and removed “see” from whenever we mention figures.

Considering merging Fig 1 and Fig 2. One subplot of these two Figures will be enough to show the difference.

Yes, we have now done so.

Google earth figures: I think it would be more appropriate to use maps or satellite images like Landsat here (<http://earthexplorer.usgs.gov/>). Further these images need, some reference frame, coordinates, a north arrow, a map where we are in Greenland.

Thanks for this. We have now switched to Landsat images with a reference frame, grid, north arrow and a map.

Figure 1: Why don't you use the transfer function of the seismometers to show the data as displacement? That will be much easier to understand for someone not that familiar with passive seismic data.

We think it is important to show the different phases of the calving event (to highlight its emergent nature), as well as to show the similarities of these signals to Amundson 2010/2012 etc. We have explained a bit more clearly what the trace is showing.

Figure 11: I don't think that Figure is necessary. It can be well seen on Figure 8.

Ok. We have removed this.

Specific comments:

For line specific comments see the attached PDF.

Thanks for your line comments too. We have adapted most of your suggestions. We have chosen to keep “emergent” as a description as this is commonly used to describe calving events (e.g. Amundson 2012, Richardson 2010) though we have now added a clearer description of what “emergent” means.

A Two-Station Seismic Method to Localize Glacier Calving Localization at Helheim Glacier Using Multiple Local Seismic Stations

M. Jeffrey Mei^{1,2,3}, David M. Holland⁴, Sridhar Anandakrishnan⁵, and Tiantian Zheng¹

¹Department of Physics, New York University Abu Dhabi, PO Box 129188, Abu Dhabi, United Arab Emirates

²Department of Applied Ocean Science and Engineering, Woods Hole Oceanographic Institution, MA 02540, United States

³Department of Mechanical Engineering, Massachusetts Institute of Technology, MA 02139, United States

⁴Courant Institute of Mathematical Sciences, New York University, 251 Mercer Street, New York, NY 10012, United States

⁵Department of Geosciences, Pennsylvania State University, University Park, PA 16801, United States

Correspondence to: Jeffrey Mei (mjmei@mit.edu)

Abstract. A ~~method of determining glacier calving location using seismic wave arrival times from paired local seismic stations is presented~~ ^{multiple-station technique for localizing glacier calving events is applied to Helheim Glacier in southeast Greenland.} The difference in ~~surface seismic~~ wave arrival times ~~for each pair~~ between each pairing of four local seismometers is used to ~~define a locus (hyperbola) of possible origin. With multiple pairs, this can be used to triangulate for the origin of the~~ seismic wave, which is interpreted as the calving location ^{generate a locus of possible event origins in the shape of a hyperbola.}

5 This method is ~~motivated by difficulties with traditional seismic location methods that fail~~ ^{used as the P- and S-waves are not distinguishable} due to the ~~proximity of the local seismometers to the event and the emergent nature of calving, which obscures the P and S-wave onsets, and the proximity of the seismometers, which combines body and surface waves into one arrival.~~ Human observed calving events are used to calibrate the seismic velocity for the method, which is then applied to other calving 10 events. Using local stations allows the calving to be localized at specific points on the glacier surface. We find that the seismic waves that arrive at the seismometers are dominated by surface (Rayleigh) waves. The surface wave velocity for Helheim Glacier is estimated using a grid search with 11 calving events identified at Helheim from August 2014 to August 2015. From this, a catalogue of 11 calving locations is generated, ~~which shows showing~~ that calving preferentially happens at the northern end of Helheim Glacier.

15 1 Introduction

The calving of marine-terminating grounded glaciers is a significant contributor to rising sea levels worldwide due to the massive volumes of ice involved that can suddenly be discharged into the sea. Depending on the ~~exact location glacier~~, the contribution ~~from of~~ calving to sea level rise can be equal to, ~~or even greater than~~, the contribution from melt processes (Rignot et al., 2013; Depoorter et al., 2013). However, the lack of understanding of the physical ~~and mathematical~~ principles that cause 20 these events means that it is difficult to precisely forecast their contribution to ~~expected~~ sea level rise in the near future ~~(e.g. Pfeffer et al. (2008), Meier et al. (2007))~~ ^(e.g. Pfeffer et al., 2008; Meier et al., 2007). Calving glaciers can ~~advance and retreat~~

in response to climate signals, ~~and this which~~ can rapidly change the sea level (Meier and Post, 1987; Nick et al., 2013). A better understanding of calving processes is vital to developing accurate predictions of sea level rise.

The lack of understanding of why and how calving events happen makes it hard to create a general ‘calving law’ (Amundson and Truffer, 2010; Bassis, 2011). Recently, seismic arrays have been deployed to monitor glaciers and to detect calving (e.g.

5 ~~Walter et al. (2013); Amundson et al. (2012)~~ (e.g. Walter et al., 2013; Amundson et al., 2012; Köhler et al., 2015). A common automated calving detection method is to take ratios of short-time-average and long-time-average seismic signals (STA/LTA). Large calving events can also generate glacial earthquakes, with surface waves detectable at a teleseismic ~~level range~~ (Nettles et al., 2008; Nettles and Ekström, 2010; Tsai and Ekström, 2007). Currently, most localization methods require visual confirmation of the calving location, unless they are sufficiently large to be seen by satellite imagery. There have not been enough direct 10 observations of ~~these~~ smaller calving events (e.g. Qamar (1988); Amundson et al. (2008)) (e.g. Qamar, 1988; Amundson et al., 2008) to identify patterns to attempt to form a general calving law. Calving events are ~~somewhat intermittent, even if they also exhibit intermittent, though they exhibit some~~ seasonality due to the seasonality of the mélange ice (~~Foga et al., 2014; Joughin et al., 2008~~, so monitoring equipment has ~~ocean temperature variations and variations in meltwater sliding~~ (Foga et al., 2014; Joughin et al., 2008). The overall unpredictability of calving requires monitoring equipment to be deployed ~~on a~~ long-term ~~in order to capture these~~ 15 basis to capture events. Automatic methods like STA/LTA can help narrow down the manual search in satellite and camera imagery for calving, but ultimately, ~~visually~~ locating a calving event requires clear weather and well-lit conditions (O’Neal et al., 2007). An exception to this is radar, but radar cannot be deployed year-round without constant refueling and swapping out of data drives, and also has problems seeing through atmospheric precipitation. Recently, high frequency pressure meters, such as Sea-Bird Electronics tsunameters, have been deployed to monitor calving at Helheim (~~Vaňková and Holland (2016), in review~~) (Vaňková and Holland, 2016).

~~In particular, land-based~~ Land-based seismometers (providing seismic data) ~~are much more useful than~~ offer improvements over simple camera or satellite imagery ~~at detecting calving~~ because seismic arrays are not limited to daylight hours, are not affected by snow, can be deployed year-round without maintenance and ~~also~~ provide quantitative data to help estimate the magnitude of calving events. Seismic studies of calving have been done at the regional (<200 km) as well as the teleseismic level.

25 Generally, teleseismic detections of calving are done via low frequency surface waves (e.g. Walter et al. (2012); O’Neal and Pfeffer (2007); while local detections are done at some ~~range~~ subset of frequencies within 1-10 Hz (e.g. Bartholomaus et al., 2012; Amundson et al., 2008).

Seismicity in glaciers has been observed for both basal processes (e.g. ~~Bartholomaus et al., 2012; Amundson et al., 2008, 2012; O’Neal~~ 30 ~~–~~

~~–~~ basal sliding) and surface processes (e.g. surface crevassing) unrelated to calving (Anandakrishnan and Bentley, 1993; West et al., 2010). Until recently, seismic signals generated by glacial calving were believed to be caused either by capsizing icebergs striking the fjord bottom (Amundson et al., 2012; Tsai et al., 2008) ~~or the sea surface~~ (Bartholomaus et al., 2012), or by sliding glaciers that speed up after calving (Tsai et al., 2008). ~~However,~~ Murray et al. (2015a) found that glacial earthquakes at Helheim Glacier are caused by glaciers temporarily moving backward and downward during a large calving event. ~~It is not yet known how to~~ 35 ~~fully categorize and characterize different calving events. For example,~~ Nettles and Ekström (2010) found that only capsizing

icebergs generate observable low-frequency surface wave energy, with calving events ~~creating tabular, wide~~ that create tabular icebergs not generating glacial earthquakes. ~~Basal crevassing has also been suggested as a mechanism (Murray et al., 2015b).~~ It is not yet known how to fully categorize and characterize different calving events.

~~Calving seismic signals~~ Seismic signals of calving events typically have emergent onsets (i.e. having a gradual increase in amplitude with no clear initial onset) with dominating frequencies around the order of 1-10 Hz (Richardson et al., 2010; O’Nel et al., 2007). The emergent ~~signals make~~ ~~nature of the signals makes~~ it hard to accurately identify a P-wave onset time, let alone a S-wave onset time, which ~~prevents~~ ~~hinders~~ the traditional seismic triangulation method that takes the ~~time~~-difference between the P- and ~~S-waves~~ ~~S-wave arrival times~~ to generate a distance to the epicenter (Spence, 1980). The other main method involves calculating backazimuths from a ratio of easting and northing amplitudes of P-waves from a broadband seismic station (e.g. Jurkevics (1988)); this also fails (e.g. Jurkevics, 1988; Köhler et al., 2015); this fails for our study due to the proximity of ~~the station~~ ~~our stations~~ and the high speed of the sound waves (4 around 3.8 km/s through ice) which makes pure ice, e.g. Vogt et al. (2008) which make the waves arrive near-simultaneously. ~~Although an emergent signal does not prevent the detection of calving as the STA/LTA method mentioned above shows, it does thwart the localization of the calving as the different seismic waves cannot be separated.~~

Another method, known as beamforming, uses the backazimuth and the different signal onset times to determine a time-delay that aligns the seismic signals coherently (Koubova, 2015). A more recent method for localizing calving events is the use of frequency dispersion ~~of surface waves~~, which uses a regional array (100-200 km away) of hydroacoustic stations to estimate a ~~range~~ ~~distance~~ between event and detector and combines this with an azimuth ~~(determined from the P-waves)~~ to create a unique intersection (Li and Gavrilov, 2008), as the stations are sufficiently far to ~~distinguish P- and S-waves~~ ~~separate different seismic wave components~~. This method has similar precision to using intersecting azimuths from two remote stations, which is enough to identify which glacier the calving occurred at, but not enough to localize the event within the glacier.

~~This motivates the creation of a more precise localization method that does not require the separation of different seismic waves. We denote this method the "Hyperbolic Method", as it uses the difference between the signal onset times at two nearby stations to generate a unique~~ In seismology, another technique to locate the epicenter of seismic events uses differences in signal arrival times to create a hyperbola, on which the event is localized. ~~Calving events were observed with the naked eye on August 12 and August 13 2014 at Helheim Glacier (in East Greenland) and on June 10 at Jakobshavn Glacier (in West Greenland). These events are used to calibrate the local surface wave velocity on the glacier surface. The Hyperbolic Method epicenter lies. This was first used in Mohorovicic (1915); Pujol (2004) notes that this method is best for shallow events where refraction along a bottom interface (glacier-rock) is insignificant. Such a technique has not yet been applied to localizing calving. The aspect ratio (vertical/vertical dimension) of Helheim Glacier is of order 0.1 and so calving events should be sufficiently shallow to use this technique. This method is limited by determining the relevant wave velocity. In our case, this is empirically determined by using hyperparameter optimization, also known as grid search (Bergstra et al., 2013). This involves exhaustively evaluating a product space of parameters to optimize some performance metric. In our case, we use a product space of surface velocity v_{eff} , x-coordinate and y-coordinate to minimize the total residual between the observed lags and the lag corresponding to each (v_{eff}, x, y) . The hyperbolic method~~ is then applied to calving events ~~at Helheim~~ using the mean v_{eff} from the grid search, to

localize the epicenters of the seismic signals generated during calving events. The grid search is then repeated with a product space of just (x, y) with the mean v_{eff} from the first grid search, and these localizations are compared to the hyperbolas.

2 Data

Four broadband seismometers (HEL1: Nanometrics Trillium 120, HEL2-HEL4: Nanometrics Trillium 240) with dual sampling rates of 40 Hz and 200 Hz were deployed around the mouth of Helheim Glacier, as seen in (Figure 1). HEL1 and HEL2 were deployed in August 2013, while HEL3 and HEL4 were deployed in August 2014. They were synchronized with Coordinated Universal Time. These stations picked up detected seismic activity from both calving as well as distant earthquakes, so we first inspect the frequency distributions of the signals to isolate calving events.

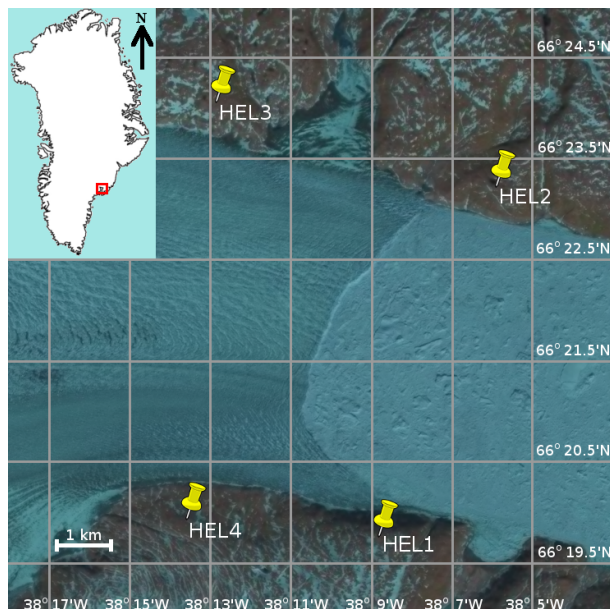


Figure 1. The four bedrock deployed seismometers deployed at Helheim Glacier as shown on Google Earth, a Landsat-8 image from July 9 2015. GPS coordinates for are referenced to WGS84. HEL1: 66°19.76'N 38°8.79'E. HEL2: 66°23.24'N 38°5.91'E. HEL3: 66°24.06'N 38°12.9'W. HEL4: 66°19.94'N 38°13.60'W. The calving front is clearly visible in between them. To the right of it Westward is Helheim Glacier; eastward is the mélange and Sermilik Fjord; to the left is Helheim Glacier.

The signals for our observed calving events match those of Amundson et al. (2012). Our observed calving event (Figure 10 2a) matches those of Amundson et al. (2012); Richardson et al. (2010); O'Neil et al. (2007) very well in both frequency distribution and shape, with an emergent onset and a power spectrum dominating in the 1-10 Hz range (see Figure 2 relatively high-frequency signals (1-20 Hz)). In contrast, teleseismic events from regional earthquakes have much lower frequency signals below 0.1 Hz. In Figure ??, we show a $M = 7.0$ earthquake that happened in Atka, Alaska, USA on August 30 2013 (<1

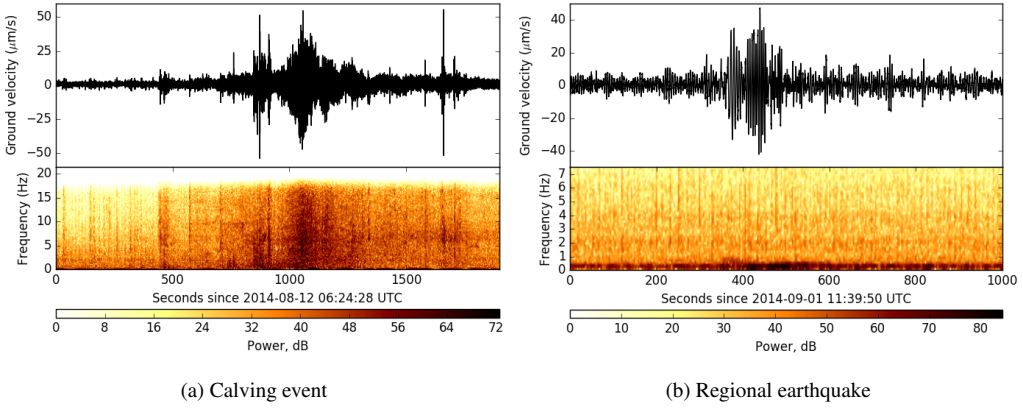


Figure 2. Spectrograms for CE-I, the (a) a calving event at Helheim on August 12 (left) 2014, and of CE-II on August 13 (right) b) a regional earthquake in 2014. The y-axis of the top panels shows counts Bárðarbunga, a dimensionless quantity showing relative ground motion of the instrument measured within the digitizing system. Iceland on September 1 2014. The easting amplitude of the seismometers is depicted here used for both events. The seismogram (top) and spectrogram (bottom) of each event share the same time axis for direct comparison. The spectrograms have a window size of 256 points (= 6.4 s).

Hz). A M5.2 regional earthquake in Bárðarbunga, Iceland on September 1 2014¹ where (Figure 2b) shows that the dominant frequencies received at the HEL seismometers are all well below 1 Hz. This means we can easily separate calving events from regional seismic activity by using a bandpass filter (Butterworth, two-pole and zero-phased). We bandpass filter between 2-18 Hz based off these spectrograms the spectrogram in Figure 2a in order to maximize the signal-to-noise ratio for our hyperbolic 5 location method. From this we are able to create a catalogue of calving events to run our Hyperbolic Method hyperbolic method algorithm. Calving events, with the exception of events in January/February 2015 for which imagery is too snow-covered to use, are confirmed with local camera imagery and MODIS satellite imagery from the Rapid Ice Sheet Change Observatory (RISCO) website².

Spectrograms for the teleseismic event from Atka, AK, United States discussed in from HEL1 (L) and HEL2 (R), showing 10 the different frequency distribution when compared to the calving event in the previous figure.

3 Localization Methods methods and Results results

3.1 Hyperbolic method

After isolating the calving events, we now present the Hyperbolic Method describe the hyperbolic method and apply it to generate a catalogue of calving locations.

15 An example of a hyperbola of equation $x^2/a^2 - y^2/b^2 = 1$, with foci at F_1 and F_2 with constant path difference $|d_2 - d_1| = 2a$.

¹See USGS Icelandic Meteorological Office record: <http://en.vedur.is/earthquakes-and-volcanism/articles/nr/2947>

²<http://www.rapidice.org/viewer/>

3.2 Hyperbolic Method

This method relies on the fact that a hyperbola can be geometrically defined as the locus (set of points) with a constant path difference relative to two foci, as seen in Figure 3. In our case, each pair of seismometers ~~aet acts~~ as foci. We need two variables to determine the path difference: the signal arrival time lag at each pair of seismometers, and the horizontal velocity of the surface waves.

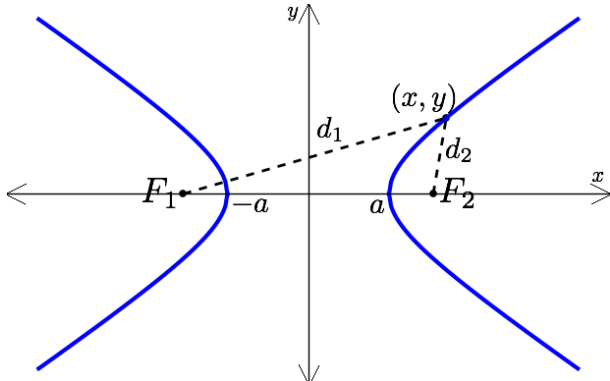


Figure 3. An example of a hyperbola of equation $x^2/a^2 - y^2/b^2 = 1$, with foci at F_1 and F_2 with constant path difference $|d_2 - d_1| = 2a$.

Assuming that the speed of seismic waves across Helheim does not vary horizontally, the signals from a calving event that happened exactly at the midpoint of the two seismometers (or ~~indeed, any any other~~ point along the perpendicular bisector of the two seismometers) would ~~register arrive~~ simultaneously at the two seismometers. Similarly, if the event happened closer to HEL1, the seismic waves would arrive slightly earlier to HEL1, and the locus of possible calving locations would instead be the set of all points whose distance from HEL1 is shorter than HEL2 by a fixed length. ~~This length is 2a as seen in Figure 3, which would be~~ (Figure 3), which is the product of the speed of the waves through the glacier (v_{seismic}) and the time lag in signal arrival (Δt). ~~This difference of 2a and~~ is defined for a hyperbola with equation $x^2/a^2 - y^2/b^2 = 1$: see Figure 3. We may use the time lag of the signal arrivals at the two seismometers (which become the foci of the hyperbola) to determine the path difference of the signals, and from this deduce the locus of possible signal sources to form the locus. One of the arms (in Figure 3, curves) (either the left curve or the right curve) of the hyperbola or right in Figure 3) may always be eliminated, as we can always see as we know which seismometer the event was closer to by seeing which station has the first signal onset. This remaining arm will intersect occurred closer to. Each time lag therefore generates one curve that intersects uniquely with the calving front, which will give the location of the calving. If the calving front is not known, using multiple pairings of the four stations, the calving location can be estimated using triangulation the calving event can be triangulated using additional pairings of other stations.

One key unknown in this method is-

This method requires evaluating the time lag between the signal arrival times at each seismometer (Figure 4), and obtaining the speed of the seismic waves through the glacier. We do not attempt to identify whether the seismic waves are P, S or surface

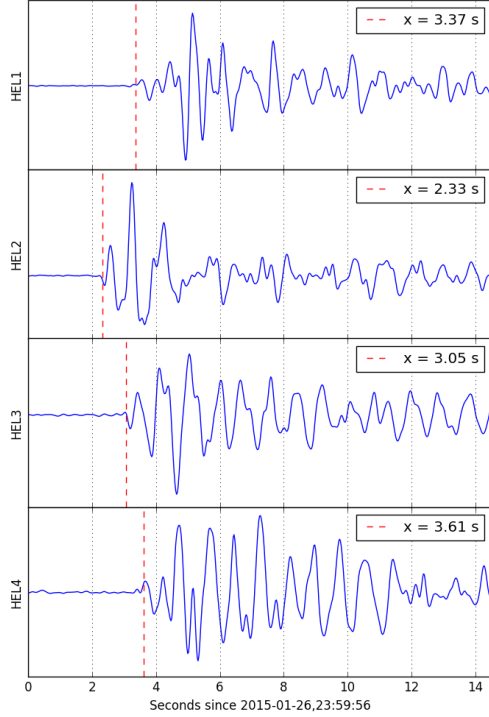


Figure 4. Seismic signals for a calving event at Helheim Glacier on January 26, 2015. The signal onset times are determined using an automated script that searches for the first instance of a gradient exceeding a particular threshold as defined in Section 3.2. The differences in the wave onset times is then used to generate a characteristic path difference for each hyperbola.

waves, except to note that it appears that there is a mixture of all of these. As the surface waves travel over a topography unique to each glacier, we rename the variable as v_{eff} , which is the effective speed of the seismic packet over the surface of Helheim Glacier using the above assumptions.

3.2 Identifying signal lags

5 To identify the time lag, we first try using cross-correlation of the signals. For subpanels HEL2 and HEL4 in Figure 4, cross-correlation gives 1.5 s, which is a plausible value by eye, but for subpanels HEL3 and HEL4, cross-correlation gives 2.2 s which is not plausible by eye. The signals in Figure 4 do look qualitatively different for HEL3 and HEL4, and it is possible that this is what prevents cross-correlation from generating an accurate lag time. Instead of using cross-correlation, we use an automated script that searches through the signal for the first instance of a raw waveform gradient exceeding 1.44

10 standard deviations of all gradients at each time step of 0.025 s (corresponding to the sampling frequency of 40 Hz). This value of 1.44 was empirically determined as this produced the closest match to cross-correlation for signals that were qualitatively similar enough to use cross-correlation. We do

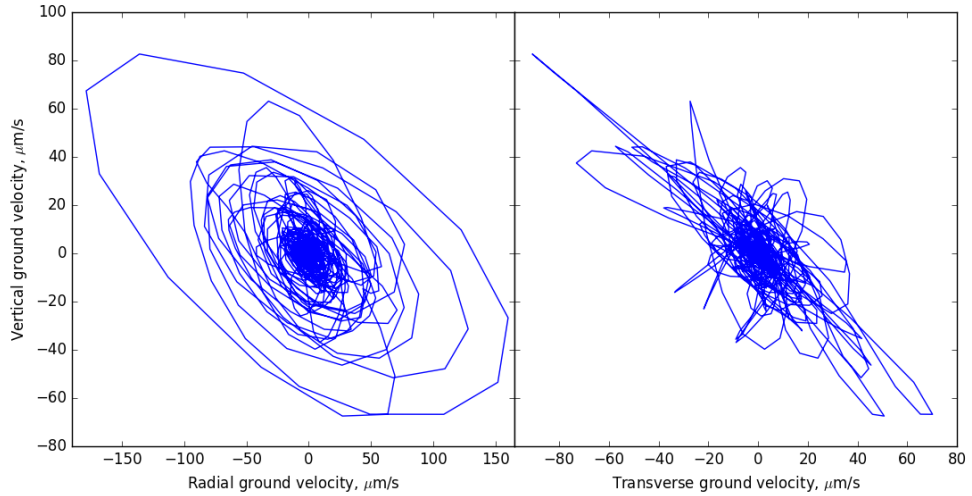


Figure 5. Particle plots of seismic wave arrivals for the calving event of July 7 2015, split into radial and transverse components. The characteristic elliptic shape of the surface Rayleigh wave is clearly visible in the radial component of the particle plot.

3.3 Determining seismic wave velocity with grid search

From particle plots (Figure 5), we know these signals are dominated by Rayleigh (surface) waves. We assume that the seismic wave travels at the same lateral speed from the epicenter (the vertical projection of the true seismic source to the surface) calving epicenter to each station. The dependence of wave speed on glacier depth is not important for this method as long 5 as the effective (surface) lateral speed to each seismometer is the same in each direction via symmetry from the source. We also assume that the glacier surface, calving epicenter and seismometers are all coplanar, so that the hyperbolas can be kept two-dimensional for simplicity. In reality, there is some elevation between the seismometers and the glacier surface, though this distance (<300 m) is so much shorter than the seismometer separation (>6500 m so 6000 m) that refraction at the ice/rock boundary is likely negligible for characterizing the hyperbola. However, this method would become more powerful precise 10 with three-dimensional hyperboloids instead of two-dimensional hyperbolas.

This method therefore requires evaluating the time lag between the signal arrival times at each seismometer (see Figure 4), and obtaining the speed of the seismic waves through the glacier. As we are not distinguishing whether the seismic waves are body or surface ones, we rename the variable as v_{eff} , which is the effective speed of the seismic packet through the glacier surface using the above assumptions.

15 To identify the time lag, we first try using cross-correlation of the signals. However, as seen in Figure 4, the signals are sometimes too different to generate an accurate lag time. For the top two subplots, the cross-correlation gives 0.47 s, which is a plausible value by eye, but for the panels HEL2 and HEL3, cross-correlation gives a value of 2.4 s, which is not plausible by eye. Instead of using cross-correlation, we use an automated script that searches through the signal for the first instance of a slope exceeding 44% of the standard deviation of all slopes at for a time step of 0.025 s (corresponding to the sampling

frequency of 40 Hz). This value of 44% was empirically determined as this produced the closest match to cross-correlation for signals that were qualitatively similar.

To calibrate the seismic velocity v_{eff} , we use two events that were observed locally at Helheim in August 2014 (with only two seismometers) as well as one event at Jakobshavn Glacier in West Greenland (where there is a similar setup with three seismometers) in June 2015. In both cases, the approximate seismic velocity corresponding to the observed location of calving was $1.17 \pm$ Using a grid search parametrizing between $1.00 < v_{\text{eff}} < 1.40$ km/s (step size 0.01 km/s) and the coordinate span of the entire map in Figure 1 (step size 1 pixel) for our 11 identified calving events, we get a mean $v_{\text{eff}} = 1.20$ km/s with a standard deviation $\sigma = 0.1$ km/s (see Figure ??). For all further plots, we therefore use $v_{\text{eff}} = 1.17$ s. The standard error for these 11 samples is therefore $\sigma/\sqrt{11} = 0.03$ km/s. For all further plots, we therefore use $v_{\text{eff}} = 1.20$ km/s. We generate four hyperbolas, using HEL1-HEL2, HEL1-HEL3, HEL2-HEL4 and HEL3-HEL4 as these have the greatest distance of ice between the stations, as we require that the rock has a negligible contribution to the wave arrival times.

Once we generate four hyperbolas, we may take their intersection to be an estimate of the calving area, as seen in Figure ???. Applying this to our entire catalogue of calving events (excluding four out of fifteen due to unclear and noisy signal onsets), we have Figure 7.

3.4 Localization results

A calving event (yellow diamond) at Jakobshavn Glacier in West Greenland as shown by Google Earth. The black circle indicates the uncertainty of the observed calving location. The same method as at Helheim is used to generate a time lag of signal onset, which is combined with a range of seismic velocities to determine which hyperbola pair intersects closest to the observed location. Note that the satellite imagery here does not show an up-to-date depiction of the calving front, and so the calving event falsely appears to originate in the

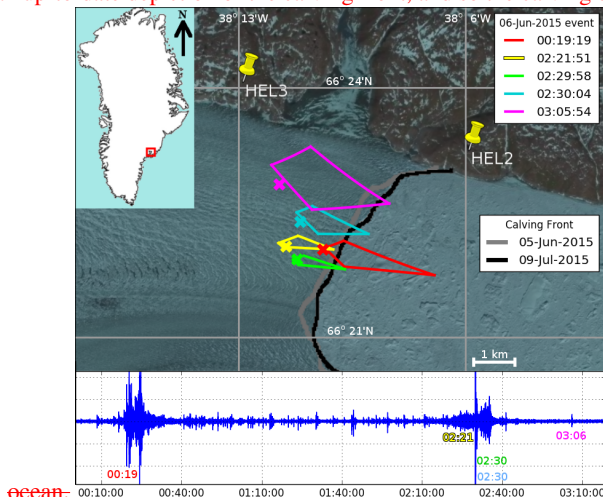


Figure 6. The calving event from June 6 2015, with the localizations (top panel) and the easting amplitudes of seismometer HEL1 (bottom panel) showing several sub-events. The x's indicate locations derived from using a grid search through a lattice of all points on the map with a fixed $v_{\text{eff}} = 1.20$ km/s.

Seismic signals for a calving event at Helheim Glacier on September 2, 2014. The signal onset times are determined using an automated script that searches for the first instance of a gradient exceeding a particular threshold as defined in the text. The differences in the wave onset times is then used to generate a characteristic path difference for each hyperbola.

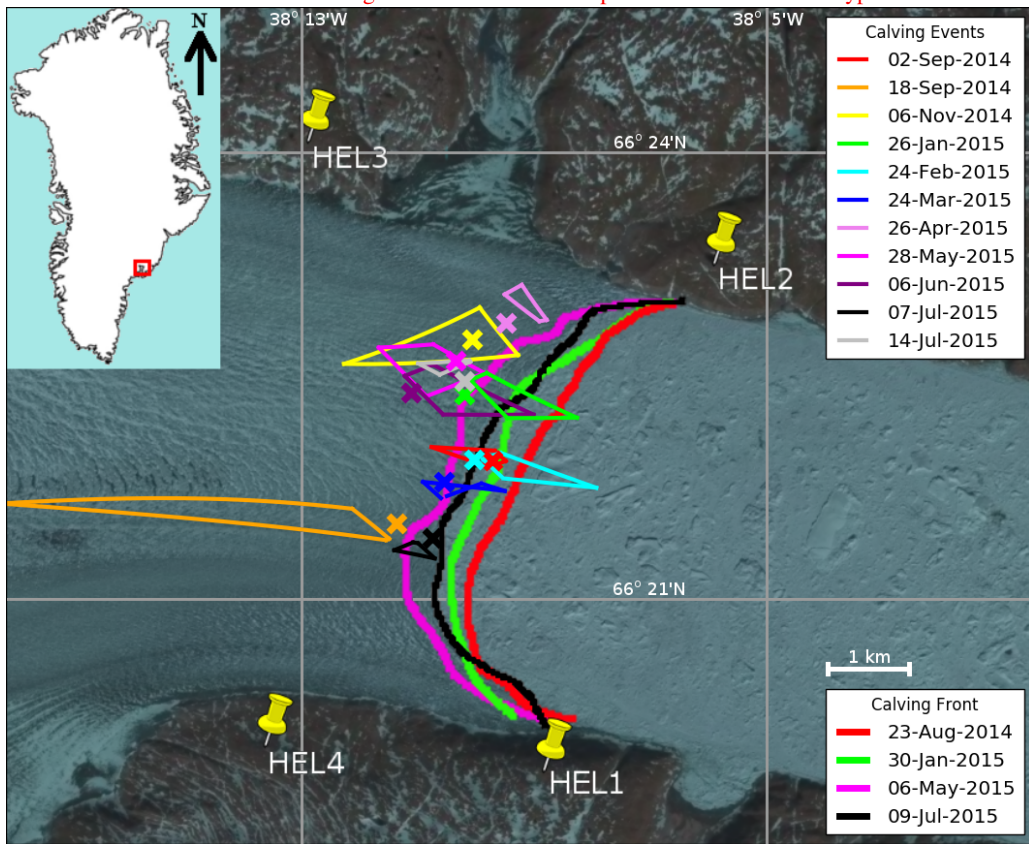


Figure 7. Catalogue of all calving events with clear signal onsets at Helheim Glacier from August 2014-August 2015 overlaid on Landsat-8 imagery of Helheim Glacier. Each color corresponds to a calving event, with only the area of overlap of the four hyperbolas being depicted. The x's represent the same event located using a grid search technique.

Hyperbolas corresponding to four pairings of seismometers with signal lags as seen in Figure 4. Of the six possible pairings of four seismometers, we use HEL1-HEL2, HEL1-HEL3, HEL2-HEL4 and HEL3-HEL4 as these have the greatest distance between the stations to improve precision and also avoid traversing large areas of rock as in the HEL2-HEL3 and HEL1-HE4 pairings. The overlapping area, shown here in red, is assumed to be the location of the calving event. The centroid of the overlapping area is indicated with a red 'x'. Once we generate four hyperbolas we may take their intersection to be an estimate of the calving area. In Figure 6, we show the progression of one calving event on June 6 2015. From this, the main peak (blue) corresponding to the highest amplitude signal is taken as a representative location for the entire event for the purposes of creating a catalogue of all events from August 2014-August 2015. Applying this method to our entire catalogue of 11 calving

events, we have Figure 7. We also re-run our grid search method, this time with a fixed $v_{\text{eff}} = 1.20$, as a check of our localization results.

4 Discussion

4.1 Interpretation of Results

The hyperbolic method and grid search method give very similar localizations for calving events at Helheim. Qualitatively, Figure 6 shows that calving propagates up-glacier, with an initial event near the calving front (red) and subsequent seismic signals originating from locations further up the glacier. The locations of events also diverge, as after the second event (yellow), the third and fourth events (green and blue) go in opposing directions. Given that the calving front depicted in grey corresponds to one day before the calving event, the fact that the first event (red) is localized so close to the calving front is a good indicator that the event is localized correctly. Similarly, the year-long catalogue in Figure 7 has events being localized near the calving front. For example, the black event of July 7 2015 is localized, for both the hyperbolic method and grid search method, immediately adjacent to the black calving front corresponding to July 9 2015. Moreover, local camera imagery also shows substantial ice loss on July 7 2015 on the southern half of Helheim Glacier. We are therefore confident that the hyperbolic method and grid search method are valid methods to localize calving.

Based on Figure 7, calving appears to cluster in the northern portion of Helheim Glacier. This is consistent with the topography of the bedrock at Helheim (Figure 8), where the northern half is on the order of ~ 200 m deeper than the southern half (Leuschen and Allen, 2013). It is possible that the deeper the ice, the higher the freeboard of the ice front and the greater the stresses that affect the calving front. In Figure 7, we see wider gaps between crevasses in the north of the glacier as compared to the south. This may also mean that the surface velocities are different in each half, which would affect the localization results. The topographic differences of both the glacier surface and ice bottom may contribute to why we see calving primarily in the northern half of Helheim.

It is possible to constrain the fault size of the rupture caused by calving. Using a shear model from Brune (1970), the radius r_0 of a circular fault is inversely proportional to the corner frequency f_c of a S-wave and is given by

$$r_0 = \frac{K_c \beta_0}{2\pi f_c}$$

5 Discussion

The Hyperbolic Method where β_0 is the shear velocity and K_c is a constant, equal to 2.34 for Brune's source model (Gibowicz and Kijko, 2000).

From Figure 9, the corner frequency is approximately bounded between 5 and 10 Hz. Taking a Poisson ratio of 0.3 for ice (Vaughan, 1995), the ratio of the Rayleigh wave velocity to S-wave velocity is approximately 0.930 (Viktorov, 1970), giving a value of $\beta_0 = 1.29$ km/s. For this rough calculation, we assume that the corner frequency is the same for the Rayleigh and S waves. This bounds the fracture size of the calving event between 48 m and 96 m. Brune's relationship does not depend on properties of the material like effective stress σ or rigidity μ . Our range of 48 - 96 m is considerably smaller than a typical observed calving fracture by around one order of magnitude. A fracture size of order 1 km would require a corner frequency of order 0.1 - 1 Hz, which we do not observe. 100 m is more on the order of a crevasse, which also occur during/before events, so it

Catalogue of all calving events with clear signal onsets at Helheim Glacier from August 2014–August 2015 overlaid on Google Earth imagery of Helheim Glacier. Each color corresponds to a calving event, with only the area of overlap as shown in Figure ?? depicted. Note that the calving front is shown only for July 2014.

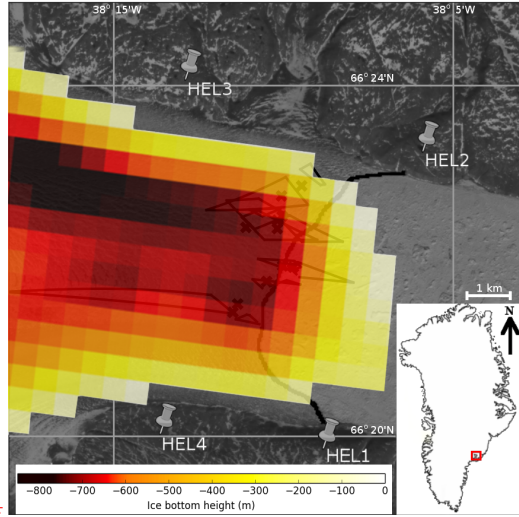


Figure 8. The calving events from Figure 7 overlaid with the bedrock topography from the Multichannel Coherent Radar Depth Sounder (MCoRDS) L3 data set from NSIDC (Leuschen and Allen, 2013), with the calving front from July 09 2015 in black. The topography is collated and averaged from 2008 to 2012.

Particle plots of surface wave arrivals for the calving event of July 7 2015, split into radial and transverse components. The characteristic elliptic shape of the Rayleigh wave is clearly visible in the radial component of the particle plot.

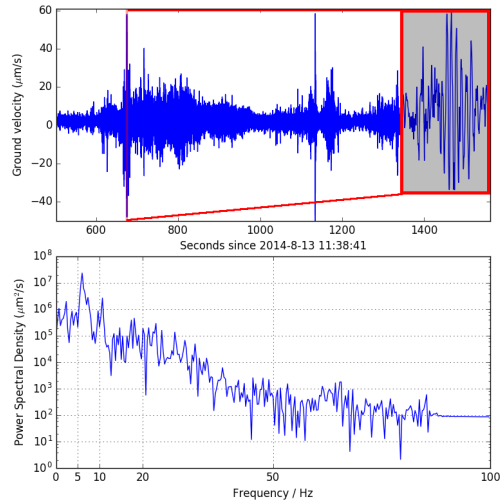


Figure 9. A typical power spectrum for a calving event (August 13 2014), for a 3-second time window containing the highest peak amplitude of the event. The shaded inset in the top panel shows a zoomed-in view of this window.

is possible that crevassing events continue to happen during the calving event and obscure the power spectrum seen in Figure 9. Both basal crevassing (e.g. Murray et al., 2015b; James et al., 2014) and surface crevassing (e.g. Benn et al., 2007) have been suggested as calving mechanisms. Murray et al. (2015b) found that calving at Helheim in 2013 was dominated by buoyant flexure via basal crevasses. Our estimated rupture sizes using Brune's model could plausibly be the size of either the basal or 5 surface crevassing. As our method assumes a planar glacier surface, we cannot distinguish whether the crevassing is at the base or the surface.

4.1 Discussion of methods

The [hyperbolic method](#) described in this paper offers ~~a powerful alternative~~ [some benefits](#) to traditional seismic location techniques, which are more suited for regional seismic arrays that can distinguish between the different seismic wave types (e.g. 10 O'Neal et al. (2007)) (e.g. O'Neal et al., 2007). Moreover, [these distant regional](#) arrays do not give the kind of precision that local arrays would have, as small errors on a regional azimuth translate to a large area of uncertainty on the local glacier surface. The [Hyperbolic Method](#) [hyperbolic method](#) takes advantage of the stations' proximity to calving events and does not require separating out the different wave phases, thus [solving sidestepping](#) the P-wave identification problem that hampered localization techniques from Amundson et al. (2008) and Richardson et al. (2010).

15 The method also offers advantages over traditional calving detection methods, which require the use of a local camera and/or satellite data to visually confirm that calving took place. As seen in (Amundson et al., 2012) Amundson et al. (2012, 2010), calving generates a characteristic seismic signal, ~~which we also see in Figures 2 and ??, where we directly compare teleseism with calving and note that teleseism does not have any energy above 5 Hz or so and have most of their energy <1 Hz~~ (Figure 2) that is easily distinguishable from signals from regional earthquakes. This is likely because higher frequency signals ~~are~~ 20 ~~severely~~ from regional earthquakes are attenuated by the time they reach the seismometers; ~~in any case, this means that seismometers can~~. This allows seismometers to be used to monitor glaciers and quickly identify calving when power in the 2-18 Hz range exceeds some ratio above the ambient noise. Importantly, this monitoring could take place year-round, during the night and also cloudy days, ~~thus replacing~~ making it a helpful addition to locating calving alongside satellite imagery, camera imagery and radar monitoring ~~as the primary method for locating calving~~.

25 The seismic ~~wave detected here does not appear to be a P-wave. Its speed of 1.17 km/s is much lower than would be expected for a P-wave in ice, which is typically larger than 3 km/s (e.g. 3.25 km/s in O'Neal et al. (2007) or 3.8 km/s in Robinson (1968)). Moreover, the particle plots in Figure 5 clearly signals detected during calving events are clearly dominated by surface waves. Particle plots (Figure 5)~~ show the characteristic elliptical shape of a Rayleigh wave (~~a surface wave~~). The Rayleigh waves, which are in theory parallel to the vertical axis, appear slanted in Figure 5. It is possible that the mix of different wave phases 30 (e.g. Love waves, also a surface wave) has ~~sheared interfered~~ the Rayleigh wave such that it is no longer parallel to the vertical axis. ~~In any case, the lack of a linear polarization (There is also a lack of linear polarization as would be expected for a P-wave) is clear. This means that the wave packet is likely dominated by surface waves. Our estimated S-wave velocity, using a Poisson ratio of 0.3, is 1.29 km/s from above. This is lower than the 1.9 km/s for S-waves in pure ice that Kohnen (1974) found. Given our characteristic surface wave velocity on the order of 1 km/s with frequencies of the order of order~~ 10 Hz (see Figure 2), this

corresponds to a surface wavelength of order 100 m, which. This is small enough to be affected by crevasses along the surface of the glacier which are of ~~depths of order 50 m~~ similar depths (Bassis, 2011). This means that we can reasonably expect these ~~air-filled~~ crevasses to affect the ~~surface~~ seismic wave velocity, ~~making our reported speed of 1.17~~ which could slow the S-waves and surface waves, ~~making our surface wave speed of 1.20~~ km/s a plausible value.

5 Because we are only working with surface waves, this limits our localization technique to just the epicenter of a calving event, with no suggestion of a focal depth. This means we could not distinguish between basal or surface crevassing, even if we could estimate a rupture size in the previous section. Moreover, we have assumed a planar ice front for simplicity. We cannot, at this point, use this method to locate any events happening below the glacier surface. It is possible that this method could be extended to determine the depth at which calving (or crevassing) occurs by using a 3-D hyperboloid instead of 2-D hyperbolas.

10 However, the main limitation of this is that the density of glaciers changes with depth and so the seismic wave speed itself should be a function of depth, and so the locus of possible origins would ~~not form a hyperbola~~ have a more complicated shape.

The calculation method we have used ignores the presence of the rock between the glacier and the seismometers, as the proximity of the seismometers to the glacier ~~makes the time the wave spends travelling across rock negligible compared to the time spent on the glacier. The localization of edge events, for which the rock surface contributes a greater proportion of the path of the surface wave~~, are not significantly affected by including the rock medium into the surface velocity calculation. However, our means that the time taken for the wave to propagate through rock is negligible. Our method does not take into account the refraction at the ice-rock interface. Again, due Due to the ice dominating the wave path from the source to the seismometers, we ~~may~~ assume that the refraction has a negligible affect on the azimuthal measurement. The rock also gives elevation to the seismometers, so that a linearly polarized P-wave would also have some vertical component. However, we do not see linear polarization in our particle plots in Figure 5.

Calving appears to preferentially happen at the northern end of trajectory of the surface waves.
The main source of error comes from identifying the signal onset. Picking out the signal onset is not fully automated. Local stations that are right by the calving front at Helheim. This is consistent with the topography of the bedrock at Helheim as seen in Figure 8, where the northern half is on the order of \sim 200 m deeper than the southern half (Leuschen and Allen, 2013). It is possible that the deeper the ice, the higher the freeboard of the ice front and the greater the stresses that affect the calving front. Camera imagery further suggests a structural difference between the northern and southern halves of Helheim, as seen in Figure ??, where there are wider ridges in the north (left side of image) as compared to the south. This may also mean that the surface velocities are different in each half, which would affect the localization results. The topographic differences of both the ice surface and ice bottom may contribute to why we see calving primarily in the northern half of Helheim.

30 The calving events from Figure 7 shown with the bedrock topography from NSIDC IceBridge MCoRDS (Leuschen and Allen, 2013) over From depth soundings made in the mélange we know that the depth is approximately 600 m, and from the MCoRDS overflight of the ice front we know that some of the ice upstream of the ice front is deeper than 600 m, and so we only show depth values that are near or below 600 m.

35 Helheim Glacier viewed from the air; the left side of the image is north and the right side of the image is south. Image provided by the Geological Survey of Denmark and Greenland.

It is possible to constrain the fault size of the rupture caused by calving. Using a shear model from Brune (1970), the radius r_0 of a circular fault is inversely proportional to the corner frequency f_c of a S-wave is given by

$$r_0 = \frac{K_c \beta_0}{2\pi f_c}$$

A typical power spectrum for the two observed calving event in August 2014, for the time period indicated between the two red lines. The shaded inset in each subplot shows the zoomed-in view of the section of the seismic trace that was used to make the power spectrum.

where β is subject to much more noise than regional arrays. While some of the noise can be filtered out, a lot of the shear velocity, K_c is a constant, equal to 2.34 for Brune's source model (Gibowicz and Kijko, 2013). From Figure 9, the corner frequency is approximately bounded between 2.5 and 10 Hz. Using a shear velocity of 1.3 km/s (given that the Rayleigh wave velocity is typically 92% of the S-wave velocity as per Sheriff and Geldart (1995)), this bounds the fracture size of the calving event between 48 m and 194 m. This relationship does not depend on properties of the material like effective stress σ or rigidity μ . This is somewhat smaller than a typical observed calving fracture by around one order of magnitude. 100 m is more on the order of a crevasse, which also occur during/before events, so it is possible that crevassing events continue to happen during the calving event and obscure the power spectrum seen in Figure 9. It is also possible that calving events are a sequence of small cracks on the order of 100 m that quickly cascade *en masse* into a larger event. A fracture size of order 1 km would require a corner frequency of order 0.1–1 Hz, which we do not observe. noise still occurs in the 2–18 Hz range that also contains most of the power from the calving signal. Moreover, as the calving events are occur between the stations, this means that the signals that arrive at each station come from different directions and may not necessarily be similar in shape. As a result, cross-correlation does not always work for determining lags. Our empirical method of using gradients is not robust and requires manual confirmation; this also means the error is difficult to quantify as the true signal onset time is not known. However, the v_{eff} of the surface waves can be estimated using a grid search method, giving plausible results. With more calving detections, the standard error of the optimized v_{eff} value will decrease. As cross-correlation does work for some events, with a sufficiently large number of calving events, we may simply discard events that do not cross-correlate correctly. This would make it possible to create an event catalogue using only automated methods.

5 Conclusions

Our results show that there are ways to get around the emergent P-wave problem for glacial calving, which prevents traditional seismic location methods, via the development of a hyperbolic method that simply measures the time delay in the signal arrival times at two seismometers. This model can be made more complex by using hyperboloids of revolution in place of calving can be localized with local seismic stations. We find that the hyperbolas, which would also give insight into the depth of the calving location local seismic signals are dominated by surface (Rayleigh) waves, and that the differences between these signal onsets can be used to localize calving. This offers an alternative to regional arrays, which can distinguish different wave phases but have lower resolution of localization. Identifying the signal onsets can be automated, but still requires manual confirmation of results. Further study should be done in determining why cross-correlation only works for a subset of the events. With

three ~~seismometers, triangulation becomes possible, and~~ ~~or more seismometers,~~ calving events can be detected and ~~located even without triangulated even without any~~ satellite or camera imagery. ~~This method can be automated for spectra with good signal-to-noise spectra, but signal onset detection of noisy spectra still requires manual inspection at this point.~~ Our catalogue of calving events at Helheim suggests that ~~calving typically initiates in the 2014-2015 season, calving typically initiated~~ at the northern half of the calving front, which will help to constrain model simulations of glacier dynamics at Helheim. ~~This technique can be applied to localize calving events at other glaciers.~~

Acknowledgements. The fieldwork necessary to collect this seismic data was made possible by the Center for Global Sea Level Change, grant G1204 of the NYU Abu Dhabi Research Institute and the Undergraduate Research Fund at NYU Abu Dhabi. Denise Holland provided the field logistics support in Greenland. ~~The authors also acknowledge the support of the Arctic Division of the Office of Polar Programs under grants ARC-0806393 and ARC-1304137. Technical installations were performed by Paul Carpenter and Jason Hebert of PASSCAL Instrument Center. The authors would like to thank Jason Amundson, Anja Diez and an anonymous reviewer for their helpful comments in improving the manuscript.~~

References

Amundson, J. M. and Truffer, M.: A unifying framework for iceberg-calving models, *Journal of Glaciology*, 56, 822–830, 2010.

Amundson, J. M., Truffer, M., Lüthi, M. P., Fahnestock, M., West, M., and Motyka, R. J.: Glacier, fjord, and seismic response to recent large calving events, Jakobshavn Isbræ, Greenland, *Geophysical Research Letters*, 35, doi:10.1029/2008GL035281, <http://dx.doi.org/10.1029/2008GL035281>, 2008.

5 Amundson, J. M., Fahnestock, M., Truffer, M., Brown, J., Lüthi, M. P., and Motyka, R. J.: Ice mélange dynamics and implications for terminus stability, Jakobshavn Isbræ, Greenland, *Journal of Geophysical Research: Earth Surface* (2003–2012), 115, doi:10.1029/2009JF001405, 2010.

10 Amundson, J. M., Clinton, J. F., Fahnestock, M., Truffer, M., Lüthi, M. P., and Motyka, R. J.: Observing calving-generated ocean waves with coastal broadband seismometers, Jakobshavn Isbræ, Greenland, *Annals of Glaciology*, 53, 79–84, doi:10.3189/2012AoG60A200, url="http://www.ingentaconnect.com/content/igsoc/agl/2012/00000053/00000060/art00010",, 2012.

Anandakrishnan, S. and Bentley, C.: Micro-earthquakes beneath Ice Streams B and C, West Antarctica: observations and implications, *Journal of Glaciology*, 39, 455–462, 1993.

15 Bartholomaus, T., Larsen, C., O’Neil, S., and West, M.: Calving seismicity from iceberg–sea surface interactions, *Journal of Geophysical Research: Earth Surface*, 117, 2012.

Bassis, J. N.: The statistical physics of iceberg calving and the emergence of universal calving laws, *Journal of Glaciology*, 57, 3–16, 2011.

Benn, D. I., Hulton, N. R., and Mottram, R. H.: ‘Calving laws’, ‘sliding laws’ and the stability of tidewater glaciers, *Annals of glaciology*, 46, 123–130, 2007.

20 Bergstra, J., Yamins, D., and Cox, D. D.: Making a Science of Model Search: Hyperparameter Optimization in Hundreds of Dimensions for Vision Architectures., *ICML* (1), 28, 115–123, 2013.

Brune, J. N.: Tectonic stress and the spectra of seismic shear waves from earthquakes, *Journal of geophysical research*, 75, 4997–5009, 1970.

Chen, X., Shearer, P., Walter, F., and Fricker, H.: Seventeen Antarctic seismic events detected by global surface waves and a possible link to calving events from satellite images, *Journal of Geophysical Research: Solid Earth* (1978–2012), 116, doi:10.1029/2011JB008262, <http://dx.doi.org/10.1029/2011JB008262>, 2011.

25 Depoorter, M., Bamber, J., Griggs, J., Lenaerts, J., Ligtenberg, S., van den Broeke, M., and Moholdt, G.: Calving fluxes and basal melt rates of Antarctic ice shelves, *Nature*, 502, 89–92, 2013.

Foga, S., Stearns, L. A., and van der Veen, C.: Application of satellite remote sensing techniques to quantify terminus and ice mélange behavior at Helheim Glacier, East Greenland, *Marine Technology Society Journal*, 48, 81–91, doi:10.4031/MTSJ.48.5.3, <http://dx.doi.org/10.4031/MTSJ.48.5.3>, 2014.

30 Gibowicz, S. J. and Kijko, A.: An introduction to mining seismology, vol. 55, Elsevier, 2013.

James, T. D., Murray, T., Selmes, N., Scharrer, K., and O’Leary, M.: Buoyant flexure and basal crevassing in dynamic mass loss at Helheim Glacier, *Nature Geoscience*, 7, 593–596, 2014.

Joughin, I., Howat, I., Alley, R. B., Ekstrom, G., Fahnestock, M., Moon, T., Nettles, M., Truffer, M., and Tsai, V. C.: Ice-front variation and tidewater behavior on Helheim and Kangerdlugssuaq Glaciers, Greenland, *Journal of Geophysical Research: Earth Surface* (2003–2012), 35 113, doi:10.1029/2007JF000837, 2008.

Jurkevics, A.: Polarization analysis of three-component array data, *Bulletin of the Seismological Society of America*, 78, 1725–1743, http://epsc.wustl.edu/~ggeuler/reading/cam_noise_biblio/jurkevics_1988-bssa-polarization_analysis_of_three-component_array_data.pdf, 1988.

Köhler, A., Nuth, C., Schweitzer, J., Weidle, C., and Gibbons, S. J.: Regional passive seismic monitoring reveals dynamic glacier activity on Spitsbergen, *Svalbard, Polar Research*, 34, 2015.

Kohnen, H.: The temperature dependence of seismic waves in ice, *J. Glaciol.*, 13, 144–147, <http://adsabs.harvard.edu/abs/1974JGlac..13..144K>, 1974.

Koubova, H.: Localization and analysis of calving-related seismicity at Kronebreen, Svalbard, https://www.duo.uio.no/bitstream/handle/10852/45791/7/final_thesis.pdf, 2015.

10 Leuschen, C. and Allen, C.: IceBridge MCoRDS L3 Gridded Ice Thickness, Surface, and Bottom, Version 2, Helheim, NASA DAAC at the National Snow and Ice Data Center, doi:<http://dx.doi.org/10.5067/YP1PVPR72IHG>., 2013.

Li, B. and Gavrilov, A.: Localization of Antarctic ice breaking events by frequency dispersion of the signals received at a single hydroacoustic station in the Indian Ocean, *The Journal of the Acoustical Society of America*, 123, 2990–2990, doi:<http://dx.doi.org/10.1121/1.2932527>, <http://scitation.aip.org/content/asa/journal/jasa/123/5/10.1121/1.2932527>, 2008.

15 Meier, M. and Post, A.: Fast tidewater glaciers, *Journal of Geophysical Research: Solid Earth* (1978–2012), 92, 9051–9058, doi:[10.1029/JB092iB09p09051](https://doi.org/10.1029/JB092iB09p09051), 1987.

Meier, M. F., Dyurgerov, M. B., Rick, U. K., O’Neel, S., Pfeffer, W. T., Anderson, R. S., Anderson, S. P., and Glazovsky, A. F.: Glaciers dominate eustatic sea-level rise in the 21st century, *Science*, 317, 1064–1067, doi:[10.1126/science.1143906](https://doi.org/10.1126/science.1143906), 2007.

Mohorovicic, A.: Die bestimmung des epizentrum eines nahbebens, *Gerl. Beitr. z. Geophys.*, 14, 199–205, 1915.

20 Murray, T., Nettles, M., Selmes, N., Cathles, L., Burton, J., James, T., Edwards, S., Martin, I., O’Farrell, T., Aspey, R., et al.: Reverse glacier motion during iceberg calving and the cause of glacial earthquakes, *Science*, 349, 305–308, 2015a.

Murray, T., Selmes, N., James, T. D., Edwards, S., Martin, I., O’Farrell, T., Aspey, R., Rutt, I., Nettles, M., and Baugé, T.: Dynamics of glacier calving at the ungrounded margin of Helheim Glacier, southeast Greenland, *Journal of Geophysical Research: Earth Surface*, 120, 964–982, 2015b.

25 Nettles, M. and Ekström, G.: Glacial earthquakes in Greenland and Antarctica, *Annual Review of Earth and Planetary Sciences*, 38, 467, 2010.

Nettles, M., Larsen, T., Elósegui, P., Hamilton, G. S., Stearns, L. A., Ahlstrøm, A. P., Davis, J., Andersen, M., de Juan, J., Khan, S. A., et al.: Step-wise changes in glacier flow speed coincide with calving and glacial earthquakes at Helheim Glacier, Greenland, *Geophysical Research Letters*, 35, 2008.

30 Nick, F. M., Vieli, A., Andersen, M. L., Joughin, I., Payne, A., Edwards, T. L., Pattyn, F., and van de Wal, R. S.: Future sea-level rise from Greenland’s main outlet glaciers in a warming climate, *Nature*, 497, 235–238, doi:[10.1038/nature12068](https://doi.org/10.1038/nature12068), 2013.

O’Neel, S. and Pfeffer, W.: Source mechanics for monochromatic icequakes produced during iceberg calving at Columbia Glacier, AK, *Geophysical Research Letters*, 34, 2007.

O’Neel, S., Marshall, H., McNamara, D., and Pfeffer, W.: Seismic detection and analysis of icequakes at Columbia Glacier, Alaska, *Journal of Geophysical Research: Earth Surface* (2003–2012), 112, doi:[10.1029/2006JF000595](https://doi.org/10.1029/2006JF000595), 2007.

Pfeffer, W. T., Harper, J., and O’Neel, S.: Kinematic constraints on glacier contributions to 21st-century sea-level rise, *Science*, 321, 1340–1343, doi:[10.1126/science.1159099](https://doi.org/10.1126/science.1159099), 2008.

Pujol, J.: Earthquake location tutorial: graphical approach and approximate epicentral location techniques, *Seismological Research Letters*, 75, 63–74, 2004.

Qamar, A.: Calving icebergs: A source of low-frequency seismic signals from Columbia Glacier, Alaska, *Journal of Geophysical Research: Solid Earth* (1978–2012), 93, 6615–6623, doi:10.1029/JB093iB06p06615, 1988.

5 Richardson, J. P., Waite, G. P., FitzGerald, K. A., and Pennington, W. D.: Characteristics of seismic and acoustic signals produced by calving, Bering Glacier, Alaska, *Geophysical Research Letters*, 37, doi:10.1029/2009GL041113, 2010.

Rignot, E., Jacobs, S., Mouginot, J., and Scheuchl, B.: Ice-shelf melting around Antarctica, *Science*, 341, 266–270, 2013.

Robinson, E. S.: Seismic wave propagation on a heterogeneous polar ice sheet, *Journal of Geophysical Research*, 73, 739–753, doi:10.1029/JB073i002p00739, 1968.

10 Sheriff, R. E. and Geldart, L. P.: *Exploration seismology*, Cambridge university press, 1995.

Spence, W.: Relative epicenter determination using P-wave arrival-time differences, *Bulletin of the Seismological Society of America*, 70, 171–183, <http://bssa.geoscienceworld.org/content/70/1/171.short>, 1980.

Tsai, V. C. and Ekström, G.: Analysis of glacial earthquakes, *Journal of Geophysical Research: Earth Surface* (2003–2012), 112, 2007.

Tsai, V. C., Rice, J. R., and Fahnestock, M.: Possible mechanisms for glacial earthquakes, *Journal of Geophysical Research: Earth Surface* 15 (2003–2012), 113, doi:10.1029/2007JF000944, 2008.

Vaňková, I. and Holland, D. M.: Calving Signature in Ocean Waves at Helheim Glacier and Sermilik Fjord, East Greenland, *Journal of Physical Oceanography*, 2016.

Vaughan, D. G.: Tidal flexure at ice shelf margins, *Journal of Geophysical Research: Solid Earth*, 100, 6213–6224, 1995.

Viktorov, I. A.: *Rayleigh and Lamb waves: physical theory and applications*, Plenum press, 1970.

20 Vogt, C., Laihem, K., and Wiebusch, C.: Speed of sound in bubble-free ice, *The Journal of the Acoustical Society of America*, 124, 3613–3618, 2008.

Walter, F., Amundson, J. M., O’Neel, S., Truffer, M., Fahnestock, M., and Fricker, H. A.: Analysis of low-frequency seismic signals generated during a multiple-iceberg calving event at Jakobshavn Isbræ, Greenland, *Journal of Geophysical Research: Earth Surface* (2003–2012), 117, doi:10.1029/2011JF002132, 2012.

25 Walter, F., Olivieri, M., and Clinton, J. F.: Calving event detection by observation of seiche effects on the Greenland fjords, *Journal of Glaciology*, 59, 162–178, doi:10.3189/2013JoG12J118, <http://dx.doi.org/10.3189/2013JoG12J118>, 2013.

West, M. E., Larsen, C. F., Truffer, M., O’Neel, S., and LeBlanc, L.: Glacier microseismicity, *Geology*, 38, 319–322, 2010.